Freezing of Molecular Motions probed by Cryogenic Magic-Angle-Spinning NMR

Supporting Information

Maria Concistrè, Elisa Carignani, Silvia Borsacchi, Ole G. Johannessen, Benedetta Mennucci, Yifeng Yang, Marco Geppi and Malcolm H. Levitt

S1. Sample

The sample studied in the present work was purchased from Sigma–Aldrich Chimica Srl (Milan, Italy) and used after exposure to atmospheric humidity for at least 4 hours. The crystal structure of the sample was checked by XRPD data recorded by Prof. Paola Paoli, Dr. Patrizia Rossi and Dr. Eleonora Macedi at University of Florence.

In figure 1s the X-Ray Powder Diffraction (XRPD) pattern of the IBU-S utilized for the solid-state NMR analysis is reported. The pattern is well comparable with the theoretical one obtained by using the single crystal data retrieved in the CSD for the racemic IBU-S dihydrate [Zhang, Y.; Grant, D.J.W. *Acta Cryst.* **2005**, *C61*, m435]. This indicates that the salt used in the present work has the same crystalline form characterized by Zhang and Grant. The XRD study and the dehydration issue are object of a separate study in course of submission. Data from DSC and TGA confirm that the loss of the water molecules occurs at about 353 K in an open pan but SSNMR spectra indicate that the loss of water does not occur in a closed rotor.

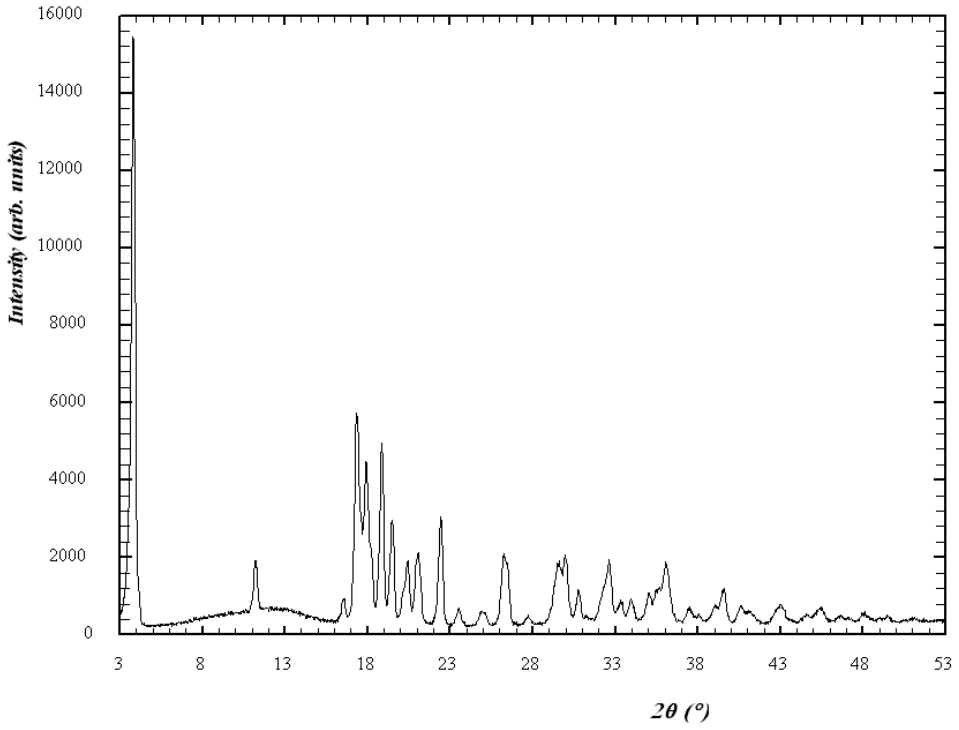

Figure 1s. XRPD spectrum of IBU-S (sodium (*RS*)-2-(4-(2-methylpropyl)phenyl) propanoate dihydrate).

S2. Solid State NMR experiments: experimental details and full series of spectra

Table 1s. Experimental details of the spectra reported in figure 2 of the manuscript. For the different ranges of temperature, the number of scans (ns), the target spinning frequency $(\omega_r/2\pi)$, the probe and the outer diameter of the rotor used, the frequency of the field used in continuous wave decoupling, the sample mass, the static magnetic field (B_0) and the cooling sytem are specified.

Series	Temp (K)	ns	$(\omega_r/2\pi)$ (kHz)	Probe	Rotor outer diameter	Decoupling field freq. (kHz)	Sample mass (mg)	B_0 (T)	Cooling system
I	358- 298	80	6.0±0.01	CP-MAS Standard	7.5 mm	42	240	9.4	none
II	283 -224	80	5.0±0.01	CP-MAS Standard	7.5 mm	50	240	9.4	Exchange dewar with ethanol + liquid N_2
III	239 - 139	80	5.0±0.02	CP-MAS modified	4.0 mm	70	150	9.4	Exchange dewar with liquid N_2
IV	120-100	32	9.0±0.02	CP-MAS custom-built	2.0 mm	75	1.5	14.1	Custom built cryogenic boiler with supercritical He
	80-40	16	9.0±0.02			75	1.5	14.1	
	20	8	9.0±0.02			75	1.5	14.1	

For spectra of **series I** and **II,** the temperature was reached heating and cooling from room temperature, respectively. For series I, after each spectrum the temperature was changed in about 5 minutes and stabilized for 15 minutes before a new acquisition. For series II, the temperature of 283 was reached in about 20 minutes, then after each spectrum the temperature was changed in about 15 minutes and stabilized for 15 minutes before a new acquisition. The sample temperature was calibrated before every experimental session by measuring the ^{207}Pb chemical shift of $Pb(NO_3)_2$ under the same experimental conditions as those used for IBU-S.

For spectra of **series III** a MAS NMR equipment developed by the Southampton group and allowing experiments down to 90 K was used [Concistrè, M.; Gansmüller, A.; McLean, N.; Johannessen, O. G.; Marín Montesinos, I.; Bovee-Geurts, P. H. M.; Verdegem, P.; Lugtenburg, J.; Brown, R. C. D.; DeGrip, W. J.; Levitt, M. H. *J. Am. Chem. Soc.* **2008**, *130*, 10490–1]. In this system, a stream of nitrogen gas is passed through a heat-exchange dewar filled with liquid nitrogen and sent to the NMR probe via a well-insulated transfer line and a custom-built variable-temperature bore insert (VT). To reduce thermal losses the bearing and drive nitrogen gas streams are cooled by bringing them into thermal contact with the cold VT gas. The magnet bore is kept warm by a flow of nitrogen purge gas.
The temperature of 239 K was reached cooling from room temperature in about 30 minutes. After each spectrum the temperature was changed in about 10 minutes and stabilized for 15 minutes before a new acquisition.
The sample temperature was calibrated before every experimental session by measuring the ^{207}Pb chemical shift of $Pb(NO_3)_2$ under the same experimental conditions as those used for IBU-S.

For spectra of **series IV** the cryogenic MAS NMR apparatus designed and built in Southampton was used [Concistrè, M. et al. *Acc.Chem. Res.* **2013**, 46, 1914-1922 (2013); Beduz, C. et al. *Proc. Natl.*

Acad. Sci. U. S. A. **2012**, *109*, 12894–8]. This system allows a minimum sample temperature of 9.6 K and a maximum spinning frequency of 15 kHz. In this equipment, the three gas streams for sample cooling (VT), and for spinning (bearing and drive) are generated from a pressurized vessel of supercritical He, and transported to the probe through a custom-built superinsulated triple-core transfer line. The cold supercritical He is filtered and divided into three separate streams, which are individually controlled by fine cryogenic needle valves to control the VT, bearing and drive gas flows independently. A set of electrical heaters allows the temperature of the three streams to be adjusted independently. The probe is housed in a brass cryostat that fits inside the room-temperature shim tube of a 14.1 T 89 mm bore magnet. The probe is inserted from above. The probe contains a modified spinner module for 2 mm outer-diameter rotors. The rotor drive tips were modified in order to hold tight at cryogenic temperatures.
The temperature of 120 K was reached cooling from room temperature in about 1 hour. After each spectrum the temperature was changed in about 10 minutes and stabilized for 15 minutes before a new acquisition. The sample temperature has been previously calibrated by using ^{127}I spin-relaxation time constant in CsI [Sarkar, R.; Concistrè, M.; Johannessen, O. G.; Beckett, P.; Denning, M.; Carravetta, M.; Al-Mosawi, M.; Beduz, C.; Yang, Y.; Levitt, M. H. *J. Magn. Reson.* **2011**, *212*, 460–3].

In figures 2s-5s the full series of spectra recorded at different temperatures are shown. The letters used for peak assignment refer to figure 6s.

We remark that continuous wave decoupling was used here only for simplicity and that the better resolution given by more advanced decoupling schemes would not have affected the conclusion. The use of modest decoupling power was chosen to avoid arcing problem. The precision of the spinning angle is not know at the lowest temperatures, therefore some of the line broadening might be due to a misset from the magic angle.

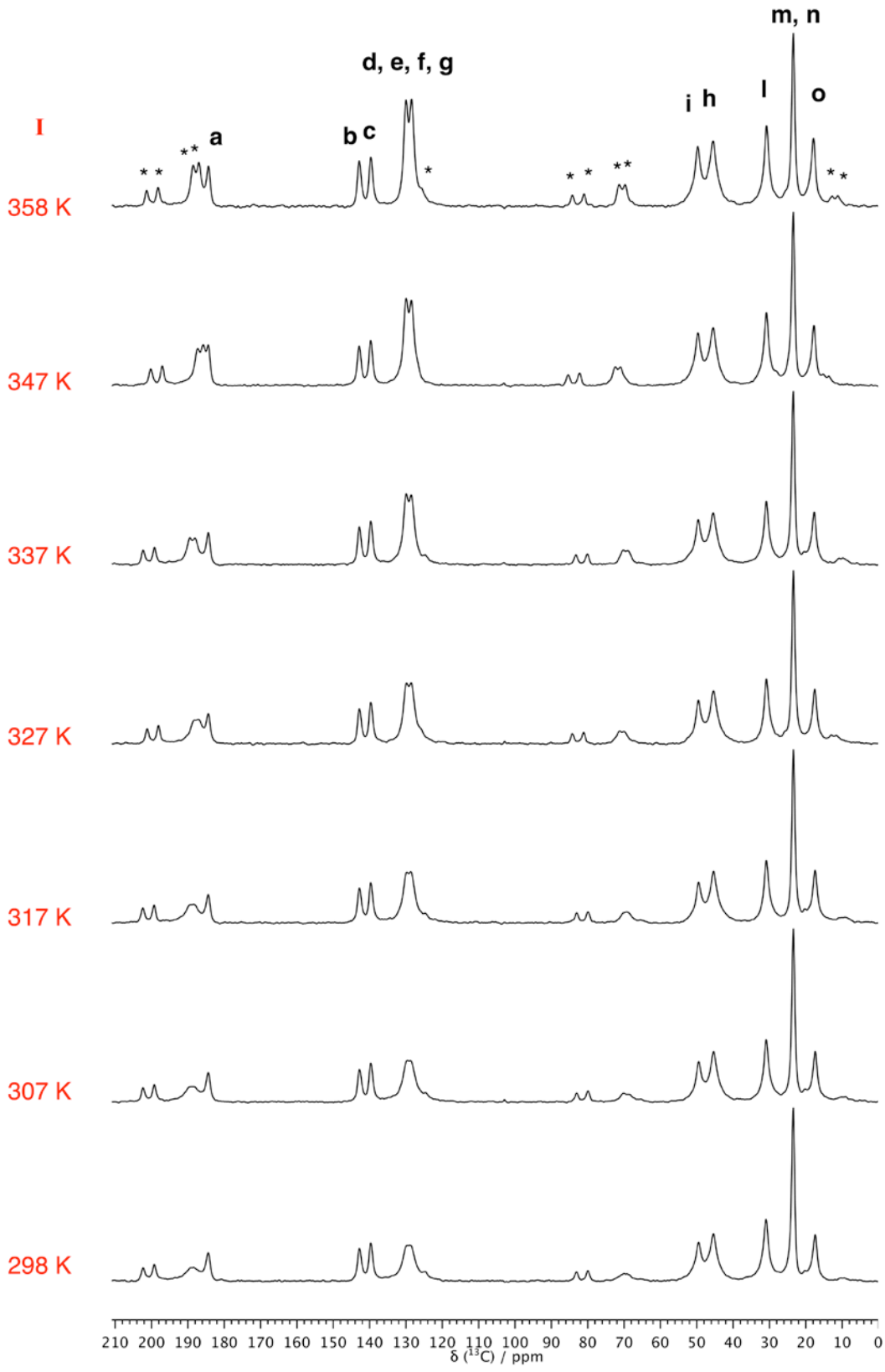

Figure 2s. ^{13}C CP-MAS spectra of IBU-S acquired in the temperature range from 358 K to 298 K (Series I). The spectra were recorded at a magnetic field of 9.4 T and magic angle spinning target frequency of 6 kHz. The actual spinning frequencies slightly vary at different temperatures and in particular they are: 6000 ± 10 Hz for spectra at 298, 307, and 317 K; 5880 ± 10 Hz for the spectrum at 327 K; 5990 ± 10 Hz for the spectrum at 337 K; 5790 ± 10 Hz for the spectrum at 347 K; 5900 ± 10 Hz for the spectrum at 358 K. All the experimental details are reported in Table 1s. Spinning sidebands are marked with asterisks.

Figure 3s. ^{13}C CP-MAS spectra of IBU-S acquired in the temperature range from 283 K to 224 K (Series II). The spectra were recorded at a magnetic field of 9.4 T and magic angle spinning frequency of 5000 ± 10 Hz. All the experimental details are reported in Table 1s. Spinning sidebands are marked with asterisks.

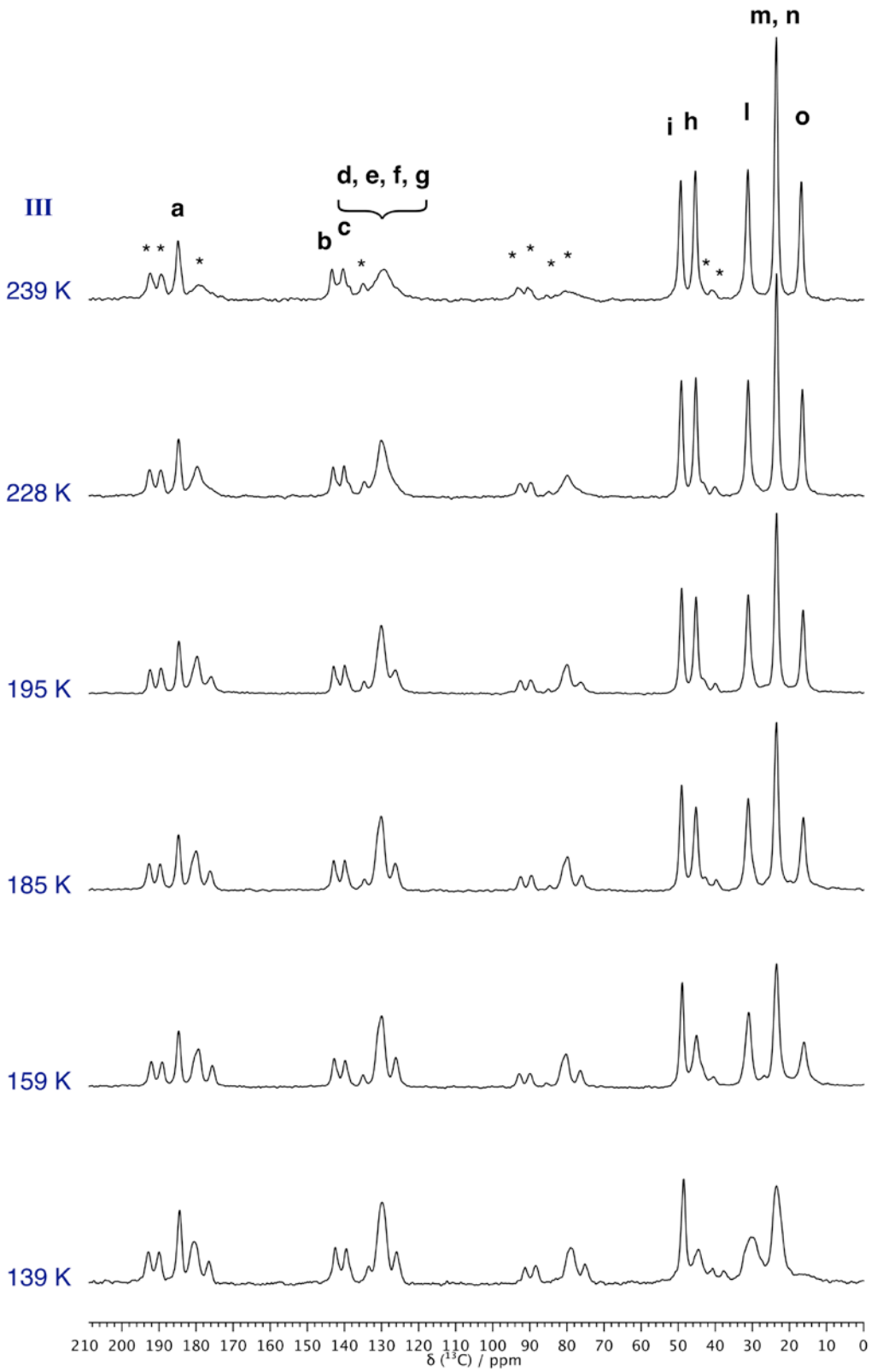

Figure 4s. ^{13}C CP-MAS spectra of IBU-S acquired in the temperature range from 239 K to 139 K (Series III). The spectra were recorded at a magnetic field of 9.4 T and magic angle spinning target frequency of 5.0 kHz. In particular the actual spinning frequency is 5000 ± 20 Hz for all the spectra except that at 139 K for which it is 5080 ± 20 Hz. All the experimental details are reported in Table 1s. Spinning sidebands are marked with asterisks.

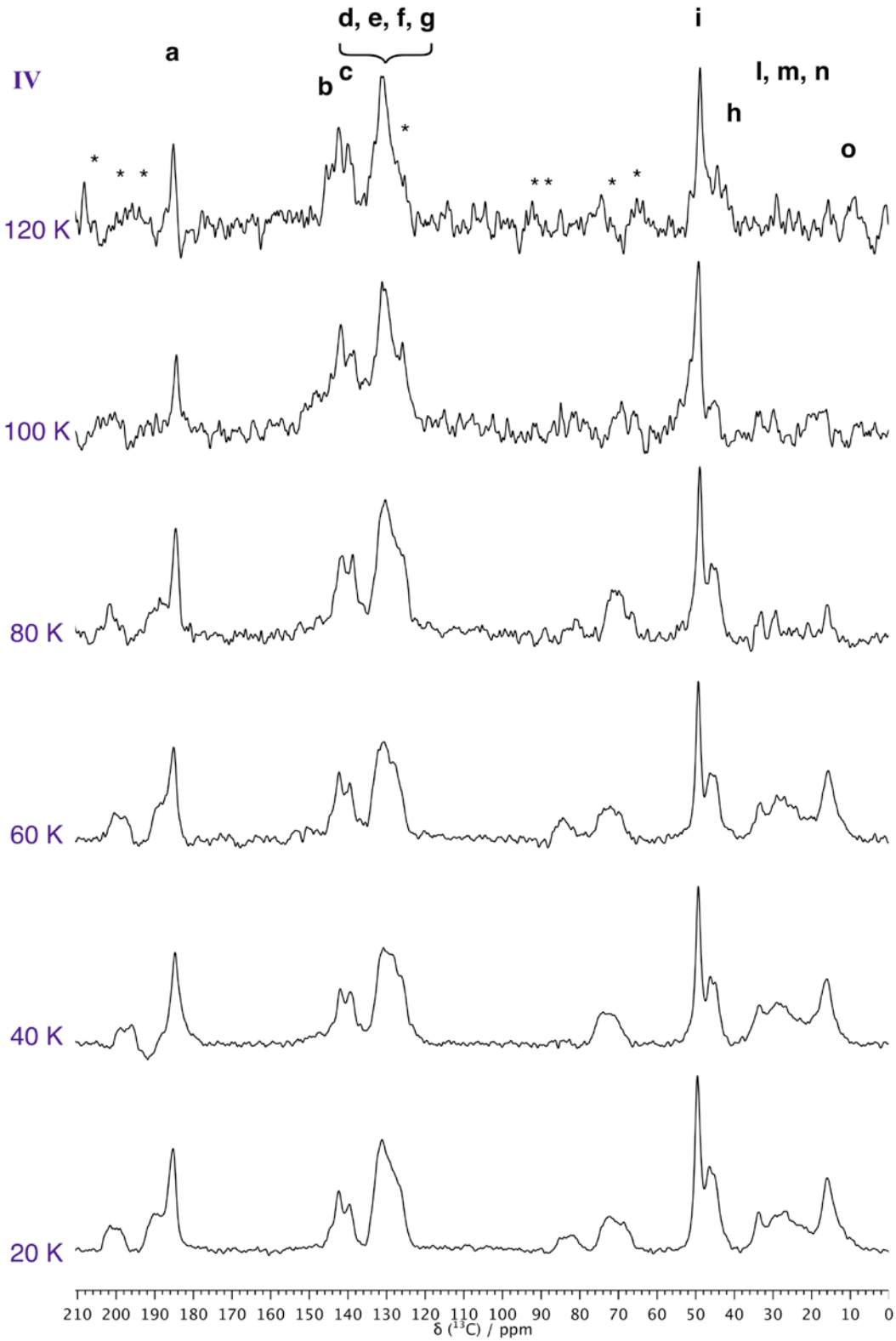

Figure 5s. ^{13}C CP-MAS spectra of IBU-S acquired in the temperature range from 120 K to 20 K (Series IV). The spectra were recorded at a magnetic field of 14.1 T and magic angle spinning target frequency of 9.0 kHz. The actual spinning frequencies slightly vary at different temperatures and in particular they are: 9100 ± 20 Hz for spectra at 120 and 100 K; 8500 ± 20 Hz for the spectrum at 80 K; 8800 ± 20 Hz for the spectrum at 60 K; 8700 ± 20 Hz for the spectrum at 40 K; 8900 ± 20 Hz for the spectrum at 20 K. All the experimental details are reported in Table 1s. Spinning sidebands are marked with asterisks.

S3. DFT calculations of isotropic chemical shift for different conformations of the isobutyl group

^{13}C chemical shifts of nuclei **c**, **h**, **l**, **m** and **n** in different conformations were calculated using DFT methods. The molecular structure and the dihedral angles varying in the different conformations are shown in Figure 6s. In tables 2s to 6s the chemical shift values calculated for the different conformations are reported. The shadowed cells indicate the chemical shift values corresponding to conformations with an energy less than 0.84 kJ mol^{-1} above that of the minimum-energy conformation (shown in bold). These values were taken into account for the analysis.

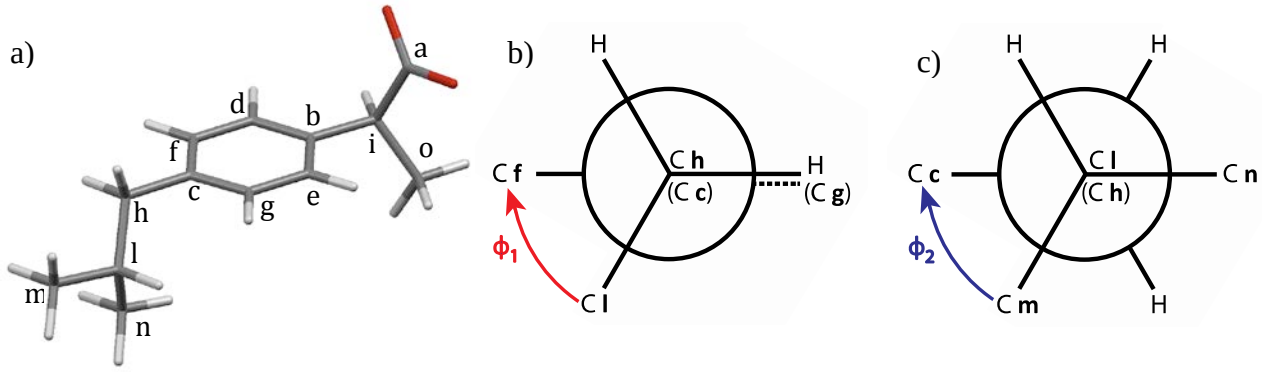

Figure 6s. a) Molecular structure of Ibuprofen and labelling of the carbon nuclei. b) Newman projection defining **l-h-c-f** dihedral angle (ϕ_1) c) Newman projection defining **m-l-h-c** dihedral angle (ϕ_2). In b) and c) when two atoms are superimposed the one written in brackets is backward.

Each conformation is defined by a pair of dihedral angles ϕ_1 and ϕ_2, corresponding to:

$$\phi_1 = \phi_1^0 + \Delta\phi_1 \qquad \text{eq. 1s}$$

$$\phi_2 = \phi_2^0 + \Delta\phi_2 \qquad \text{eq. 2s}$$

where $\phi_1^0 = 126°$ and $\phi_2^0 = 174°$ correspond to the conformation obtained form x-ray data optimizing the sole positions of hydrogens and carbons **h**, **l**, **m**, **n** (Figure 6s (a)). The different values of $\Delta\phi_1$ and $\Delta\phi_2$ are reported in tables 2s-6s.

In order to directly compare the calculated absolute shielding values with the experimentally measured isotropic chemical shifts, the following expression is used:

$$\delta_{iso} = -[\sigma_{iso} - \sigma_{ref}] \qquad \text{eq. 3s}$$

where σ_{ref} is determined with the widely used method of plotting computed shieldings against experimental shifts and fit the data with a line of slope -1. The extrapolation to zero shift gives the shielding of the reference σ_{ref} [Harris, R. K.; Hodgkinson, P.; Pickard, C. J.; Yates, J. R.; Zorin, V. *Magn. Reson. Chem.* **2007**, *45*, S174-S186.]. σ_{ref} obtained for the presented data is 180.56 ppm.

Table 2s. Chemical shift values of carbon **c** calculated for different conformations of the isobutyl group. $\Delta\phi_1$ and $\Delta\phi_2$ are defined in eqs. 1s and 2s. All the chemical shift values are reported in ppm and referred to TMS. For the geometry corresponding to the missing value in the table the calculation did not converge. The shadowed cells indicate the chemical shift values corresponding to conformations with an energy less than 0.84 kJ mol^{-1} above that of the minimum-energy conformation (shown in bold).

	$\Delta\phi_1$											
$\Delta\phi_2$	0	30	60	90	120	150	180	210	240	270	300	330
0	**143.13**	143.69	140.36	137.91	139.69	142.29	139.74	139.78	141.88	146.15	146.74	144.78
30	143.69	138.77	137.96	139.26	141.98	135.95	139.18	138.11	142.63	143.88	142.67	140.30
60	140.36	141.30	137.94	140.40	135.17	142.42	137.60	139.60	138.95	139.94	138.63	139.88
90	137.91	139.23	139.18	138.00	142.22	138.61	136.54	139.11	141.67	141.14	143.25	143.71
120	139.69		141.15	142.32	140.45	137.72	140.75	143.36	143.42	144.07	145.79	145.36
150	142.29	140.70	143.17	141.22	138.65	141.20	142.98	142.93	142.05	144.35	145.81	144.82
180	139.74	138.91	139.83	137.39	140.51	142.20	139.34	139.80	141.11	144.84	145.34	143.66
210	139.78	141.28	138.39	140.63	143.09	137.21	140.17	139.56	143.31	142.89	142.20	139.90
240	141.88	139.35	139.48	140.91	136.38	142.47	139.13	139.35	139.54	140.08	138.86	140.88
270	146.15	141.07	138.98	137.97	142.00	138.83	137.38	139.52	141.62	142.10	144.69	145.56
300	146.74	143.50	141.53	142.74	140.52	137.89	141.76	144.09	143.74	144.14	146.98	146.34
330	144.78	143.69	144.18	141.55	137.80	141.43	144.40	143.67	142.67	144.26	147.20	145.88

Table 3s. Chemical shift values of carbon **h** calculated for different conformations of the isobutyl group. $\Delta\phi_1$ and $\Delta\phi_2$ are defined in eqs. 1s and 2s. All the chemical shift values are reported in ppm and referred to TMS. For the geometry corresponding to the missing value in the table the calculation did not converge. The shadowed cells indicate the chemical shift values corresponding to conformations with an energy less than 0.84 kJ mol^{-1} above that of the minimum-energy conformation (shown in bold).

	$\Delta\phi_1$											
$\Delta\phi_2$	0	30	60	90	120	150	180	210	240	270	300	330
0	**46.53**	42.83	39.28	39.36	41.73	41.12	38.99	39.65	42.66	44.06	45.70	46.31
30	42.83	36.79	30.95	32.34	35.67	35.67	30.30	31.96	36.15	41.15	43.29	42.38
60	39.28	32.12	29.89	30.56	35.26	31.52	28.18	28.97	38.64	42.29	42.26	43.17
90	39.36	39.05	35.93	39.55	39.45	37.07	34.41	40.27	44.32	45.66	45.41	45.20
120	41.73		41.09	41.66	42.84	41.58	40.38	43.14	46.27	48.10	46.67	46.30
150	41.12	43.71	43.02	42.17	42.85	42.52	42.36	43.77	46.16	46.98	47.63	48.20
180	38.99	39.53	39.69	38.77	40.31	40.96	39.91	39.96	42.09	43.68	45.47	46.47
210	39.65	32.36	32.10	32.81	37.01	37.77	32.01	33.09	37.43	43.05	43.55	44.09
240	42.66	36.35	29.87	32.41	37.24	31.30	28.49	30.64	39.68	42.95	42.44	42.79
270	44.06	43.90	34.27	38.27	37.99	34.99	33.26	37.92	42.97	43.55	44.01	42.88
300	45.70	46.39	41.37	42.91	43.36	42.60	40.38	42.88	46.17	47.98	46.94	46.30
330	46.31	42.83	43.14	44.19	45.25	44.42	42.73	44.60	47.91	48.44	47.83	48.50

Table 4s. Chemical shift values of carbon **l** calculated for different conformations of the isobutyl group. $\Delta\phi_1$ and $\Delta\phi_2$ are defined in eqs. 1s and 2s. All the chemical shift values are reported in ppm and referred to TMS. For the geometry corresponding to the missing value in the table the calculation did not converge. The shadowed cells indicate the chemical shift values corresponding to conformations with an energy less than 0.84 kJ mol^{-1} above that of the minimum-energy conformation (shown in bold).

	$\Delta\phi_1$											
$\Delta\phi_2$	0	30	60	90	120	150	180	210	240	270	300	330
0	**34.16**	29.73	25.16	28.25	32.08	30.52	25.73	28.35	33.49	35.69	36.05	36.22
30	29.73	27.10	27.63	31.83	32.76	29.58	28.66	32.84	32.36	32.87	31.17	29.50
60	25.16	31.46	31.50	31.35	30.82	33.43	34.50	32.88	29.14	27.98	26.57	28.64
90	28.25	32.16	26.97	27.99	33.43	31.77	26.54	26.26	30.18	31.49	33.39	33.83
120	32.08		26.57	29.05	31.57	29.44	25.47	28.10	34.47	37.04	36.95	36.07
150	30.52	30.11	27.39	29.03	32.01	30.29	26.43	28.88	34.14	35.59	34.87	36.15
180	25.73	27.16	24.93	28.11	32.25	30.57	25.46	28.15	33.68	35.57	35.45	36.36
210	28.35	30.99	27.61	31.15	33.16	29.56	28.86	32.28	33.35	31.99	30.54	28.80
240	33.49	31.56	31.70	30.27	30.85	33.71	33.34	30.75	28.22	27.67	26.49	28.69
270	35.69	29.33	26.77	27.80	33.11	31.41	25.59	25.93	30.51	33.12	33.58	34.10
300	36.05	31.53	26.26	29.09	32.09	29.64	24.92	27.86	33.99	38.03	36.42	35.76
330	36.22	29.73	26.98	28.29	31.75	30.65	27.45	29.75	34.28	35.74	34.66	36.77

Table 5s. Chemical shift values of carbon **m** calculated for different conformations of the isobutyl group. $\Delta\phi_1$ and $\Delta\phi_2$ are defined in eqs. 1s and 2s. All the chemical shift values are reported in ppm and referred to TMS. For the geometry corresponding to the missing value in the table the calculation did not converge. The shadowed cells indicate the chemical shift values corresponding to conformations with an energy less than 0.84 kJ mol^{-1} above that of the minimum-energy conformation (shown in bold).

	$\Delta\phi_1$											
$\Delta\phi_2$	0	30	60	90	120	150	180	210	240	270	300	330
0	**18.67**	20.45	25.69	29.60	24.74	25.72	26.19	24.03	23.90	24.39	24.21	21.94
30	20.45	22.81	40.94	42.37	27.19	22.32	25.47	24.68	25.01	23.64	23.93	21.59
60	25.69	37.70	51.79	32.76	18.13	19.56	23.62	24.83	22.38	23.27	23.34	22.70
90	29.60	40.18	35.54	20.76	17.09	21.25	24.70	22.68	22.16	22.74	24.05	25.82
120	24.74	26.06	24.31	19.01	18.35	21.64	24.65	23.84	22.95	24.64	25.82	24.16
150	25.72		22.12	21.71	19.44	22.32	25.36	24.80	23.62	24.12	24.07	20.71
180	26.19	22.58	25.66	30.34	24.25	25.54	26.56	24.45	23.15	24.44	23.88	21.77
210	24.03	37.26	40.94	42.37	27.70	22.91	24.54	25.08	24.40	23.19	23.54	21.73
240	23.90	39.68	51.78	32.84	17.58	20.12	23.51	24.25	22.19	23.47	23.15	21.80
270	24.39	25.86	35.13	20.46	17.07	21.87	25.80	22.67	22.77	23.38	24.70	25.78
300	24.21	21.09	24.13	19.12	18.22	21.79	25.09	24.60	23.81	24.70	25.76	23.89
330	21.94	20.45	21.49	21.71	19.36	22.43	25.08	24.88	24.52	23.85	24.33	21.12

Table 6s. Chemical shift values of carbon **n** calculated for different conformations of the isobutyl group. $\Delta\phi_1$ and $\Delta\phi_2$ are defined in eqs. 1s and 2s. All the chemical shift values are reported in ppm and referred to TMS. For the geometry corresponding to the missing value in the table the calculation did not converge. The shadowed cells indicate the chemical shift values corresponding to conformations with an energy less than 0.84 kJ mol^{-1} above that of the minimum-energy conformation (shown in bold).

	$\Delta\phi_1$											
$\Delta\phi_2$	0	30	60	90	120	150	180	210	240	270	300	330
0	**24.13**	23.94	24.65	23.67	19.65	20.11	25.33	32.79	26.91	25.05	26.33	25.64
30	23.94	23.23	26.48	23.62	19.00	19.74	40.48	48.12	30.51	24.41	25.06	24.11
60	24.65	25.67	25.43	23.96	20.31	34.90	53.70	39.53	21.78	21.12	23.14	22.92
90	23.67	24.52	25.47	25.91	28.53	39.55	39.81	24.83	19.55	20.81	24.41	24.17
120	19.65	24.76	26.96	26.32	23.06	26.11	25.83	22.29	19.29	20.19	24.16	24.51
150	20.11		25.89	23.47	19.98	20.54	22.74	24.09	20.12	20.67	24.78	25.32
180	25.33	22.84	25.29	23.89	19.55	19.01	25.46	33.17	27.15	25.02	26.44	25.55
210	32.79	25.31	25.69	23.51	18.03	19.57	40.42	47.79	31.69	24.00	24.86	24.39
240	26.91	24.77	25.44	22.61	19.93	34.02	53.40	38.41	21.10	20.64	23.61	23.74
270	25.05	24.74	26.41	25.95	27.39	38.93	38.78	24.65	19.40	21.12	24.82	24.97
300	26.33	24.55	27.13	26.29	22.90	26.31	25.91	21.31	19.82	20.66	24.59	24.94
330	25.64	23.94	25.41	23.65	19.88	20.57	22.27	23.79	20.68	21.12	25.10	25.46